Enabling the Wireless Charging via Bus Network: Route Scheduling for Electric Vehicles

Yong Jin, Jia Xu, *Member, IEEE*, Sixu Wu, Lijie Xu, and Dejun Yang, *Senior Member, IEEE*

***Abstract*— The development of Electric Vehicle (EV) helps to ease energy crises and deduce vehicle exhaust emissions. However, it also brings a great impact on both transportation networks and power grids. There are some serious impediments in terms of energy charging to the popularization of EV, such as high deployment cost of charging stations, low charging efficiency, and voltage deviation of power grid. To address these issues, we design a new EV charging system, which levers the bus network in urban areas through the integration of OnLine Electric Vehicle (OLEV) system and Microwave Power Transfer (MPT) system. We formulate the EV route scheduling problem based on this new charging system to maximize the total residual energy subject to all EVs can arrive to their destinations before deadlines. Then, we propose an approximation algorithm, *RSA*, to solve the route scheduling problem. To relieve the traffic congestion, we further formulate the conflict-free EV route scheduling problem, and use the matching based algorithm, *FRSA*, to find the EV route schedules with the maximal residual energy. Through the extensive simulations, we demonstrate that *RSA* and *FRSA* can increase the average residual energy by 67.66% and 50.36% compared with the solution without the designed wireless charging system, respectively. Moreover, *RSA* reduces 22.22% of travel time and outputs 77.23% of residual energy, and *FRSA* can obtain 83.51% residual energy with 3.62% of extra travel time of the corresponding optimal solutions on average, respectively.**

***Index Terms*— Intelligent transportation system, wireless charging, electric vehicle, bus network, restricted shortest path, maximum weighted matching.**

I. Introduction

RECENTLY, EVTank and China YiWei Institute of Economics released the report of medium and long-term development prospects of global new energy vehicle market (2025) [1], which predicted that the global sales of new energy passenger vehicles will increase from 2.21 million in 2019 to 12 million in 2025, with an average annual compound growth rate of 32.6%. The passenger car market forecast compiled by Japanese research company Fuji economy [2] showed that the global sales of Electric Vehicles (EVs) would reach 22.02 million in 2035. The popularization of EVs not only reduces local carbon emissions, but also forwards the dependence on fossil-fuel to electric power from conventional power plant.

However, there are some major challenges of EV popularizations. First, the energy capacity limitation restricts the traveling distance. Significant investment cost [3] and land resources are needed for large-scale deployment of charging stations. Second, the EV users always want to arrive at the specified locations before the specified time, such as the deadline of work attendance, appointments, and meetings. In these cases, it is impossible for EV users to pay substantial time to charge their EVs before departure. Moreover, the traditional charging schemes of EVs also bring the unbalance charging demand, which causes larger voltage deviation of power grid [4].

The above issues prompt us to design the new charging system with low expense, low time cost, and predictable charging demand. Fortunately, in most cities, the public transportation system, such as bus network, is highly developed, and can cover the most tracks of people in daily life. Thus, the most of EV trajectories can be covered by the bus network in urban areas.

We propose an urban EV wireless charging system which overlays the bus network, combing the OnLine Electric Vehicle (OLEV) system [5], [6] and Microwave Power Transfer (MPT) [7]. The bus can be charged by OLEV system in moving state. The EVs can be charged by high frequency MPT with the rectified DC power of EV about 100 KW. The distance between the transmitter and receiver is not larger than 6 m with frequency of 5.8 GHz. Specially, fast charging technology, e.g., Teslas super charging station [8] is expected to be commercialized in the future to enable an EV to afford to be charged several times during its journey. Thus, the MPT charging for EVs will not affect the battery life of EVs. Moreover, an external substance detective device is equipped on the buses to detect human or animals, who are close to the bus within 1.8 m for protecting pedestrians or pets from microwave signal radiation. Furthermore, a microwave shields system [9] is deployed on EVs and buses to shield the microwave signals within the frequency range of 700 MHz to

Manuscript received February 29, 2020; revised July 10, 2020 and August 16, 2020; accepted September 8, 2020. This work was supported in part by NSFC under Grant 61872193, in part by the Postgraduate Research and Practice Innovation Program of Jiangsu Province under Grant SJKY19_0760, in part by NSF under Grant 1717315, and in part by the Natural Science Foundation of the Jiangsu Higher Education Institutions of China under Grant 19KJB520020. The Associate Editor for this article was H. Gao. *(Corresponding author: Jia Xu.)*

Yong Jin is with the Jiangsu Key Laboratory of Big Data Security and Intelligent Processing, Nanjing University of Posts and Telecommunications, Nanjing 210023, China, and also with the School of Computer Science and Engineering, Changshu Institute of Technology, Changshu 215500, China (e-mail: 2018070263@njupt.edu.cn).

Jia Xu, Sixu Wu, and Lijie Xu are with the Jiangsu Key Laboratory of Big Data Security and Intelligent Processing, Nanjing University of Posts and Telecommunications, Nanjing 210023, China (e-mail: xujia@njupt.edu.cn; 1019041115@njupt.edu.cn; ljxu@njupt.edu.cn).

Dejun Yang is with the Colorado School of Mines, Golden, CO 80401 USA (e-mail: djyang@mines.edu).

Digital Object Identifier 10.1109/TITS.2020.3023695

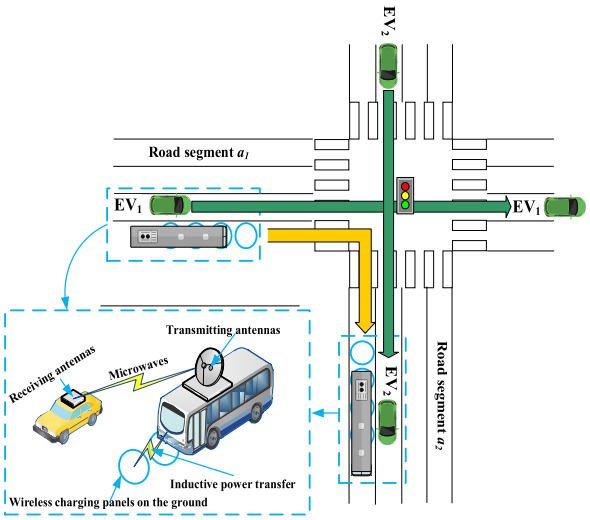

Fig. 1. Scenario of EV route scheduling with bus network assisted wireless charging.

TABLE I
MICROWAVE POWER TRANSFER FOR EVS

EV	Battery (kWh)	Consumption (kWh/km)	Ratio (%)	Distance (km)
GWM C30EV	37	0.14	5.4	14.29
CHEVROLET MENLO	52.2	0.13	3.8	15.38
Model S	75	0.13	2.7	15.38
AUDI e-tron	95	0.20	2.1	10.00

13 GHz, such as the windows and sunroof made of glass with a conducting coating or covered with plastic with a conductive coating, the seats and roof flannelette made of microwave shielding fabrics. So, we can deploy a transmitting antenna on the bus and a receiving antenna on EV. The EV can be charged by the high-power MPT when ist is close to the buses actively.

Thus, our charging system can effectively extend the traveling distance of EVs without significant investment cost and land resources. Furthermore, EVs can be charged during their journeys without extra time. Another great advantage is that the OLEV system is supported by the exclusive distribution network [5], [6] and then avoid the voltage deviation and power loss.

In Table I, shows the battery capacity (kWh), energy consumption (kWh/km), ratio of charged energy to battery capacity and increased travel distance of different EVs using MPT, when the average velocity of EVs is 25 km/h and the distance of the road segment is 0.5 km. So, the EV can obtain energy of 100 $kW \times \frac{0.5\ km}{25\ km/h}$=2 kWh from MPT. In this article, we aim to schedule EV routes in the bus network assisted wireless charging system. As illustrated in Fig. 1, there are two EVs and one bus in the charging system. Each EV has a source and a destination. The bus has its regular schedule, and is charged through OLEV system. The EVs can be charged by the bus using MPT when they are close to the bus at same road segments. For example, EV_1 can be charged by the bus at road segment a_1, and EV_2 can be charged by the bus at road segment a_2. Our goal is to find the travel path from the source to the destination for each EV to minimize the total energy cost of all EVs under the constraints of traveling time and initial energy.

Unfortunately, to the best of our knowledge, there is no off-the-shelf EV route scheduling designed for such overlay wireless charging system in the literature. There are some challenges: First, the EV route schedules should satisfy both deadline constraint and energy constraint, and the shortest path algorithm with single constraint cannot be used to solve our dual constrained problem straightforwardly. Second, the special challenge of EV route scheduling is that the traveling time and energy cost of EVs will be largely affected by the selected charging road segment in the bus routes. Moreover, if we further consider that only one EV can be charged by the same bus at the same charging road segment, the EV route scheduling problem will become more complex because the route scheduling of EVs will affect each other due to the exclusive use of charging road segments.

The main contributions of this article are as follows:

(1) We design a unique wireless charging system for EVs supported by the bus network in urban areas, which integrates the advantages of OLEV system and MPT technology. To the best of our knowledge, we are the first to study the EV route schedule problem for such overlay EV wireless charging system.

(2) We formulate the *Bus network assisted wireless charging EV Route Scheduling (BRS)* problem, and propose an approximation *Route Scheduling Algorithm (RSA)* to solve the *BRS* problem based on the approximation solution of *Restricted Shortest Path (RSP)* problem, which is a special case of *BRS* problem.

(3) To avoid charging conflict and relieve traffic congestion, we further formulate the *Bus network assisted conflict-Free EV Route Scheduling (BFRS)* problem. We present the *conflict-Free Route Scheduling Algorithm (FRSA)* to solve the *BFRS* problem through the maximum weighted matching between the EVs and the candidate routes to maximize the total residual energy of all EVs.

(4) We conduct extensive simulations for the designed algorithms. The simulation results show that *RSA* and *FRSA* can increase the average residual energy by 67.66% and 50.36% compared with the solution without the designed wireless charging system. Moreover, *RSA* reduces 22.22% of travel time and outputs 77.23% of residual energy, and *FRSA* can obtain 83.51% residual energy with 3.62% of extra travel time of the corresponding optimal solutions on average, respectively.

The rest of this article is organized as follows. Section II reviews the state-of-art research on EV route scheduling and charging optimization problem. We design the system model and formulate the *BRS* problem, as well as present approximation algorithm for the *BRS* problem in Section III. We formulate the *BFRS* problem, and propose the polynomial-time algorithm in Section VI. The simulation results are presented in Section V. We conclude this article in section VI.

II. RELATED WORK

The recent research on EV transportation mainly aimed to solve the problems of energy-optimal routing [10], [11],

charging station deployment and management [12], [16], wireless charging system [17], and charging optimization strategies [18], [19]. Some studies focused on the routing optimization of EV routing along its journey. Reference [10] formalized the EV routing problem as an instance of the shortest path problem with additional path related cost. They presented a fast routing algorithm that can handle dynamic cost and improve the time complexity. Reference [11] proposed a time and energy efficient routing algorithm to extend the travel distance and prolong the battery longevity of EVs based on historical driving data. A number of studies concluded that the deployment of charging stations is a major factor for extending the driving distance of EV. Reference [12] studied the size and locations of charging stations for EVs in traffic networks considering grid constraints to balance the charging demand and power network stability. Reference [13] proposed a reliable routing decision scheme for vehicular ad hoc networks based on the Manhattan mobility model through integrating roadside units into wireless and wired modes. Reference [14] proposed a probabilistic model of the traffic network in the form of a discrete-time Markov chain by using mobility trajectories and their statistical data. Reference [15] designed a Residual Network (ResNet)-Temporal Convolutional Network (TCN) model to predict the urban traffic volume. Zhang *et al.* [16] designed an optimal pricing scheme to minimize the service dropping rate of the charging stations. Chen *et al.* [17] designed a multiple-charger multiple-port charging system for scheduling a limited quantity of chargers to serve more Plug-in EVs (PEVs). Reference [18] presented a smart charging strategy for the PEV network, which contains multiple charging options, including *AC level 2 charging* and *DC fast charging* at charging stations. Khan *et al.* [19] presented the wireless charging utility maximization framework to maximize the utility of wireless charging units for EV charging at signalized intersections. However, the static charging at stations not only occupy lots of land resources, but also may cause the congestion at the charging stations.

In terms of EV wireless charging, Ko and Jang [20] designed the OLEV system for the mass transportation system. In [21], the authors studied the impact of wireless charging and mobility of EVs on the wholesale electricity market based on locational marginal price. Reference [22] researched the power supply architectures predominantly used for EV wireless charging, i.e., the series *LC* resonant and the hybrid series-parallel resonant full-bridge inverter topologies. A magnetic positioning approach which can solve the misalignment issue associated with wireless EV charging by sharing the wireless charging structure was proposed in [23]. In [24], the short-term operation of wireless charging station was presented by capturing the interdependence among the electricity and transportation networks. However, up to now, the investment cost of OLEV or wireless charging panel is very high for all EVs because the system will be deployed under all lanes and their maintenance is very difficult. In our charging system, we only deploy the OLEV system for bus lane with the low cost of deployment and maintenance.

Many research focused on the joint optimization of EV charging and EV routing. Reference [25] proposed both global optimal scheduling scheme and local optimal scheduling scheme for EV charging and discharging. Reference [26] proposed a mobile edge computing based system with a big data driven planning strategy of charging station selection. Reference [27] formulated a joint routing and charging scheduling optimization problem for an Internet of Electric Vehicle (IoEV) network, and proposed an approximate algorithm to achieve affordable computational complexity in large-size IoEV networks. In [28], a routing scheme was proposed to improve the experience quality of wireless charging by minimizing the relative excess time spent by mobility-on-demand-EV system customers. Reference [29] formulated the en-route charging navigation in a dynamic programming setting for both deterministic and stochastic traffic network, and proposed a charging schedule algorithm, which can reduce computational complexity.

In particular, the unpredictable mobility of EVs bring many challenges to smart grid. In [30], the authors proposed a distributed control algorithm that adapts the charging rate of EVs to the available capacity of the distribution network. Zakariazadeh *et al.* [31] proposed a multi-objective operational scheduling method for charging/discharging of EVs in a smart distribution system. Reference [32] proposed an energy management approach for the home photovoltaic systems to power the electric vehicle battery charging facility.

Our approach differs from the existing research as follows. First, in our wireless charging system, the bus can be charged by the OLEV system and EVs can be charged by the bus at the same road segments using MPT. We only need to deploy a few coils or charging panels on the bus lane, reducing the number of charging stations. Second, we aim to find the route for each EV under constraints of both deadline and energy such that the reduction of total energy cost of all EVs is maximized. Finally, we conduct the exclusive assignment between the feasible charging road segments and EVs, to avoid charging conflict and alleviate the traffic congestion. To the best of our knowledge, the mobile wireless charging assisted EV route scheduling problem based on bus network has not been studied yet.

III. Bus Network Assisted Wireless Charging EV Route Scheduling

A. System Model and Problem Formulation

We consider a set of EVs equipped with the receiving antenna of MPT traveling from their source locations to specified destinations in a transportation network. We assume that there is an underlying bus network with fixed schedule, where the buses create the energy reserves during their regular travel. The buses are charged by the OLEV system using inductive power transfer technology, and are equipped with the directed transmitting antennas of MPT. The EVs can be charged by the high-power MPT when they are close enough to the buses.

The transportation network can be characterized by a directed graph $\mathcal{G}(\mathcal{N}, \mathcal{A})$, where $\mathcal{N}$ denotes the set of n nodes, i.e., road junctions and the source/destination locations of EVs. $\mathcal{A}$ represents the set of m road segments that connect the

adjacent nodes in $\mathcal{N}$. Benefit by the advancement of dynamic charging technology [33], the charging process is transparent to the EVs, i.e., the EVs do not need to stop or even slow down in charging process. All EVs travel at a constant speed at different road segments. We don't consider the stop-and-go case of EVs. This means that the energy consumption of EVs only depends on the travel distance. We denote the set of EVs and buses by $\mathcal{V}$ and $\mathcal{B}$, respectively. Let $\mathcal{A}_\mathcal{B} \subseteq \mathcal{A}$ be the set of road segments in the bus route schedule. Let $\mathcal{A}_b \subseteq \mathcal{A}_\mathcal{B}$ be the set of road segments in the route schedule of any bus $b \in \mathcal{B}$. Our objective is to find a route p_e from the source s_e to the destination d_e fror any EV $e \in \mathcal{V}$ within deadline t_e. We assume that each bus $b \in \mathcal{B}$ travels at a constant speed r_b. Let r_e^a be the speed of EV e at any road segment $a \in \mathcal{A}$. Specifically, if a is a charging road segment, $r_e^a = r_b$ in order to synchronize the EV and bus. Let γ_e be the unit energy consumption of e. Let E_e^{max} and E_e^0 be the energy capacity of battery and the initial energy of e, respectively. The charging power of MPT is α. As an emergency charging system, we assume that each EV is charged at most once on its route. We denote the time that any bus $b \in \mathcal{B}$ enters any road segment $a \in \mathcal{A}_\mathcal{B}$ as t_b^a. Then the residual energy of e after traveling any road segment $a \in p_e$ can be calculated by:

$$E_e^a = \min\{E_e^0 - \gamma_e(|p_e^a| + |a|) + \sum_{a' \in p_e} x_e^{a'} \alpha \frac{|a'|}{r_e^{a'}}, E_e^{max}\} \quad (1)$$

where $p_e^a \subseteq p_e$ is the sub route of p_e before next road segment a. $x_e^{a'}$ is a binary variable to indicate whether e is charged at road segment a'. $x_e^{a'}$=1 if e is charged at road segment a'. $x_e^{a'}$=0 otherwise. Without loss of generality, we denote the charging road segment of e as a_e. $|a'|$ is the length of road segment a'. $|p_e^a|$ is the length of route p_e^a.

The objective of *BRS* problem is to find the route schedule $\mathcal{P}$ of all EVs to maximize the total residual energy subject to all EVs can arrive to their destinations before deadlines (if possible). Note that this objective is equivalent to minimize the total energy consumption of EVs. The *BRS* problem can be formulated as:

$$\begin{aligned} &\boldsymbol{BRS}\ \max \textstyle\sum_{e\in\mathcal{V}} E_e^a, d_e \in a, a \in p_e \\ &s.t.\ (a)\ \textstyle\sum_{a\in p_e} \frac{|a|}{r_e^a} \le t_e, \forall e \in \mathcal{V} \\ &\quad (b)\ \textstyle\sum_{a\in p_e} x_e^a \le 1, \forall e \in \mathcal{V} \\ &\quad (c)\ \Pi_{a\in p_e} E_e^a \ge 0, \forall e \in \mathcal{V} \\ &\quad (d)\ x_e^a \in \{0,1\}, \forall a \in p_e, \forall e \in \mathcal{V} \end{aligned} \quad (2)$$

The constraint (a) ensures that each EV e can reach the destination d_e before the deadline t_e. Constraint (b) ensures that each EV e is charged at most once on its route. Constraint (c) ensures that the residual energy of e is always nonnegative on its route.

We summarize the frequently used notations in Table II.

TABLE II
FREQUENTLY USED NOTATIONS

Notation	Description
$\mathcal{G}, \mathcal{P}$	transportation network, route schedule of all EVs
$\mathcal{N}, \mathcal{A}$	set of road junctions, set of road segments in $\mathcal{G}$
n, m	number of road junctions in $\mathcal{N}$, number of road segments in $\mathcal{A}$
$\mathcal{V}, \mathcal{B}$	set of EVs, set of buses
$\mathcal{A}_\mathcal{B}$	set of road segments in the bus route schedule
$\mathcal{A}_b$	set of road segments in the route schedule of bus b
s_e, d_e	source of EV e, destination of EV e
t_e	deadline of EV e
a_e	charging road segment of EV e
p_e	route from s_e to d_e for EV e before t_e
a	road segment in $\mathcal{A}$
r_e^a, r_b	speed of EV e at road segment a, speed of bus b
γ_e, α	unit energy consumption of EV e, charging power of MPT
E_e^{max}, E_e^0	energy capacity of battery of EV e, initial energy of EV e
t_b^a	time when the bus b enters road segment a
E_e^a	residual energy of e after traveling road segment a
p_e^a	sub route of p_e before next road segment $a \in p_e$
x_e^a	binary variable to indicate whether e is charged at road segment a
$\mathcal{P}_e^\mathcal{B}$	set of possible routes of EV e via one charging road segment

B. Algorithm Design

In this subsection, we present the *Route Scheduling Algorithm (RSA)* to solve the *BRS* problem. First of all, as the following theorem shows, it is NP-hard to find the optimal solution for the *BRS* problem.

Theorem 1: BRS problem is NP-hard.

Proof: Since the energy consumption of each EV is independent. The *BRS* problem is equivalent to minimize the total energy consumption for each EV. Consider the special case where every EV does not pass through the charging road segment, i.e., the constraints (2-b), (2-c), and (2-d) are removed from the problem. Then the problem is simplified to choose the shortest path from the source to the destination before deadline. This problem is *Restricted Shortest Path (RSP)* problem [34] actually. Since the *RSP* problem is a well-known NP-hard problem, the *BRS* problem is NP-hard. □

The *RSP* problem is to compute a shortest path p_e for each EV e from s_e to d_e such that the travel time is no larger than the deadline t_e. The *RSP* problem can be formulated as

$$\begin{aligned} &\boldsymbol{RSP}\ \min \textstyle\sum_{a\in p_e} |a|, \forall e \in \mathcal{V} \\ &s.t. \textstyle\sum_{a\in p_e} \frac{|a|}{r_e^a} \le t_e, \forall e \in \mathcal{V} \end{aligned} \quad (3)$$

Since the *BRS* problem is NP-hard, we turn our attention to develop an approximation algorithm. Note that each EV can be charged at most once. The *BRS* problem can be solved by considering the following two cases for each EV:

Case 1: The EV does not pass through the charging road segment. In this case, we compute the shortest path from the source to the destination before deadline for each EV. This problem is an instance of *RSP* problem, and can be solved by *Simple Efficient Approximation (SEA)* [35] with $(1+\epsilon)$-approximation.

Case 2: The EV passes through one charging road segment. In this case, we compute the shortest path from the source to the destination before deadline for each EV ahead of and behind charging road segment, respectively. Then we assemble the two paths together with the charging road segment into the integrated path for this case.

Finally, we choose the path with the minimum energy consumption from the above two cases for each EV.

The whole process is illustrated in Algorithm 1. Let $\mathcal{P}_e^\mathcal{B}$ be the set of possible routes of EV e via one charging road

Algorithm 1 *RSA*

Input: $\mathcal{G}$, $\{t_e, E_e^{max}, E_e^0, s_e, d_e, \gamma_e\}_{\forall e\in\mathcal{V}}$, $\{\mathcal{A}_b, r_b\}_{\forall b\in\mathcal{B}}$, ϵ, $\{r_e^a, t_b^a\}_{\forall e\in\mathcal{V},\ \forall a\in\mathcal{A},\forall b\in\mathcal{B}}$
Output: $\mathcal{P}$

1 $\mathcal{P} \leftarrow \varnothing$;
2 **foreach** $e \in \mathcal{V}$ **do**
3 $p_e^{\mathcal{B}} \leftarrow \varnothing$;
  // Case 1:
4 $p_e \leftarrow SEA(\mathcal{G}, t_e, \epsilon, s_e, d_e)$; $c(p_e) \leftarrow \gamma_e|p_e|$;
5 **if** $c(p_e) > E_e^0$ **then** $p_e \leftarrow \varnothing$; $c(p_e) \leftarrow \infty$;
  // Case 2:
6 **foreach** $b \in \mathcal{B}$ **do**
7 **foreach** $a_e \in \mathcal{A}_b$ **do**
8 $\overleftarrow{p_e} \leftarrow SEA(\mathcal{G}, t_b^{a_e}, \epsilon, s_e, a_e^l)$;
9 $\overrightarrow{p_e} \leftarrow SEA(\mathcal{G}, t_e - t_b^{a_e} - \frac{|a_e|}{r_b}, \epsilon, a_e^r, d_e)$;
10 $\overleftrightarrow{p_e} \leftarrow \overleftarrow{p_e} \uplus a_e \uplus \overrightarrow{p_e}$;
11 **if** $\Pi_{a\in\overleftrightarrow{p_e}} E_e^a \geq 0$ **then**
12 $c(\overleftarrow{p_e}) \leftarrow \gamma_e|\overleftarrow{p_e}|$; $c(\overrightarrow{p_e}) \leftarrow \gamma_e|\overrightarrow{p_e}|$;
13 $c(a_e) \leftarrow \gamma_e|a_e| - \min\{E_e^{max} - E_e^0 - c(\overleftarrow{p_e}), \alpha\frac{|a_e|}{r_b}\}$;
14 $c(\overleftrightarrow{p_e}) \leftarrow c(\overleftarrow{p_e}) + c(a_e) + c(\overrightarrow{p_e})$;
15 $\mathcal{P}_e^{\mathcal{B}} \leftarrow \mathcal{P}_e^{\mathcal{B}} \cup \overleftrightarrow{p_e}$;
16 $\overleftrightarrow{p_e} \leftarrow \text{argmin}_{\overleftrightarrow{p_e'}\in\mathcal{P}_e^{\mathcal{B}}} c(\overleftrightarrow{p_e'})$;
  // Choose the better one of Case 1 and Case 2:
17 **if** $\overleftrightarrow{p_e} \neq \varnothing$ **and** $c(\overleftrightarrow{p_e}) < c(p_e)$ **then**
18 $\mathcal{P} \leftarrow \mathcal{P} \cup \{\overleftrightarrow{p_e}\}$;
19 **else if** $p_e \neq \varnothing$ **then** $\mathcal{P} \leftarrow \mathcal{P} \cup \{p_e\}$;

segment. The function $c()$ returns the energy consumption of the route.

For Case 1, we adopt *SEA* to obtain the shortest path p_e from s_e to d_e before deadline t_e for each EV (Line 4).

For Case 2, we iterate every charging road segment of every bus, and compute the shortest path $\overleftrightarrow{p_e}$ via one charging road segment from the source to the destination before deadline (Lines 6-15). Specifically, the route of Case 2 is assembled by three part: the path ahead of the charging road segment $\overleftarrow{p_e}$, the charging road segment a_e, and the path behind the charging road segment $\overrightarrow{p_e}$. Let a_e^l and a_e^r be the two endpoints with the direction of bus. Path $\overleftarrow{p_e}$ can be obtained by calling *SEA* from s_e to a_e^l with deadline $t_b^{a_e}$ (Line 8). Similarly, $\overrightarrow{p_e}$ can be obtained by calling *SEA* from a_e^r to d_e with deadline $t_e - t_b^{a_e} - \frac{|a_e|}{r_b}$ (Line 9). Then the route is assembled by these three parts (Line 10), where symbol $\uplus$ represents assembling the route. If $\overleftrightarrow{p_e}$ satisfies the energy constraint, we compute the energy consumption of $\overleftrightarrow{p_e}$ (Lines 11-14), and put it into set $\mathcal{P}_e^{\mathcal{B}}$ (Line 15). After all iterations, we select the route with minimum energy consumption in $\mathcal{P}_e^{\mathcal{B}}$ as the candidate route of Case 2 (Line 16).

Finally, we choose the better one of Case 1 and Case 2 as the final schedule of EV e (Lines 17-19).

C. Algorithm Analysis

Theorem 2: RSA can output the solution in $O(|\mathcal{V}||\mathcal{B}|m^2\ n(\log\log n + \frac{1}{\epsilon}))$.

Proof: According to [35], *SEA* takes $O(mn(\log\log n + \frac{1}{\epsilon}))$ time. The running time of *RSA* is dominated by finding the restricted shortest path of Case 2 (Line 8 or Line 9), which is bounded by $O(|\mathcal{V}||\mathcal{B}|m^2\ n(\log\log n + \frac{1}{\epsilon}))$. □

Theorem 3: *RSA* can output the solution with energy consumption no more than $(1+\epsilon)(OPT + \alpha\sum_{e\in\mathcal{V}}\frac{|a_e|}{r_b})$, where OPT is the energy consumption of optimal solution. $\epsilon \in (0, 1)$ is a constant.

Proof: Since p_e is chosen from the solutions of two cases, the performance of *RSA* is determined by the worst performance of these two cases. Note that Case 1 adopts *SEA* to obtain the $1+\epsilon$-approximation solution for the *RSP* problem.

Next, we analyze the performance of Case 2. Let OPT be the energy consumption of optimal solution in Case 2. Let $OPT(e)$ be the energy consumption of optimal solution of EV e. Let $OPT_1(e)$ and $OPT_2(e)$ be the energy consumption of optimal solution in the sub-paths ahead of and behind the charging road segment a_e, respectively. Let $RSP_1(e)$ be the energy consumption of the shortest path of *RSP* problem from s_e to a_e^l with deadline $t_b^{a_e}$. Let $RSP_2(e)$ be the energy consumption of the shortest path of *RSP* problem from a_e^r to d_e with deadline $t_e - t_b^{a_e} - \frac{|a_e|}{r_b}$. Note that all possible sub-paths behind a_e are with same deadline since the charged EV has to travel after time $t_b^{a_e} + \frac{|a_e|}{r_b}$. Thus we have:

$$RSP_2(e) = OPT_2(e) \tag{4}$$

Moreover, the charged EV has to complete the travel ahead of a_e before time $t_b^{a_e}$. We have:

$$RSP_1(e) \leq OPT_1(e) \tag{5}$$

Due to $RSP_1(e) \leq OPT_1(e)$, the EV follows optimal solution may charge at most $OPT_1(e) - RSP_1(e)$ more energy than the *RSP* solution. Let OPT_c and RSP_c be the energy consumption of optimal solution and *RSP* solution at the charging road segment a_e, respectively. We have:

$$OPT_c \geq RSP_c + RSP_1(e) - OPT_1(e) \tag{6}$$

Note that *SEA* can output the $1+\epsilon$-approximation solution for the *RSP* problem. Thus, for any EV e, we have the following inequations based on (4), (5) and (6):

$$\begin{aligned} c(\overleftrightarrow{p_e}) &= c(\overleftarrow{p_e}) + c(\overrightarrow{p_e}) + c(a_e) \\ &\leq (1+\epsilon)(RSP_1(e) + RSP_2(e) + RSP_c) \\ &\leq (1+\epsilon)(OPT_1(e) + OPT_2(e) \\ &\quad + OPT_c + OPT_1(e) - RSP_1(e)) \\ &= (1+\epsilon)(OPT(e) + OPT_1(e) - RSP_1(e)) \end{aligned}$$

where the last equality relies on the fact of $OPT(e) = OPT_1(e) + OPT_2(e) + OPT_c$.

Note that $OPT_1(e) - RSP_1(e)$ is the extra energy of optimal solution charged at a_e with maximum value of $\alpha\frac{|a_e|}{r_b}$. Thus we have:

$$c(\overleftrightarrow{p_e}) \leq (1+\epsilon)(OPT(e) + \alpha\frac{|a_e|}{r_b}) \tag{7}$$

Accumulate (7) for all the EVs, we have:

$$\sum_{e\in\mathcal{V}} c(p_e) \le (1+\epsilon)(OPT + \alpha \sum_{e\in\mathcal{V}} \frac{|a_e|}{r_b})$$

Obviously, the performance of Case 2 is worse than that of Case 1. Thus *RSA* can output the solution with energy consumption no more than $(1+\epsilon)(OPT + \alpha \sum_{e\in\mathcal{V}} \frac{|a_e|}{r_b})$. □

IV. Conflict-Free EV Route Scheduling

A. Problem Formulation

However, the *charging conflict* may occur in Case 2 of the solution of *BRS* problem when multiple EVs charged by the same bus at the same charging road segment. The *charging conflict* may decrease the charging efficiency and increase the radiation to human body because the multiple pair of receiving and sending antenna of MPT working at the same road segment simultaneously will increase the microwave signal radiation range and radiation intensity. Moreover, the *charging conflict* may aggravate the traffic congestion and accident risk because several EVs need to close and follow the same bus concurrently.

To avoid *charging conflict*, we define the *BFRS* problem by adding the constraint that only one EV can be charged by the same bus at the same charging road segment. We extend the decision variable x_e^a to $x_e^{a,b}$ to indicate whether e is charged at road segment a by bus b. The *BFRS* problem can be formulated as follows:

$$\begin{aligned} &\boldsymbol{BFRS}\ \max \sum_{e\in\mathcal{V}} E_e^a, d_e \in a, a \in p_e \\ &s.t.\ (a)\ \textstyle\sum_{a\in p_e} \frac{|a|}{r_e^a} \le t_e, \forall e \in \mathcal{V} \\ &\quad (b)\ \textstyle\sum_{a\in p_e}\sum_{b\in\mathcal{B}} x_e^{a,b} \le 1, \forall e \in \mathcal{V} \\ &\quad (c)\ \textstyle\Pi_{a\in p_e} E_e^a \ge 0, \forall e \in \mathcal{V} \\ &\quad (d)\ \textstyle\Pi_{e\in\mathcal{V}} x_e^{a,b} \le 1, \forall a \in p_e, \forall b \in \mathcal{B} \\ &\quad (e)\ x_e^{a,b} \in \{0,1\}, \forall a \in p_e, \forall b \in \mathcal{B}, \forall e \in \mathcal{V} \end{aligned} \tag{8}$$

where constraint (d) ensures that only one EV can be charged by the same bus at the same charging road segment.

B. Algorithm Design and Analysis

In this subsection, we present the *conflict-Free Route Scheduling Algorithm (FRSA)* to solve the *BFRS* problem. Note that *BFRS* problem is also NP-hard since *BFRS* problem is a tighten version of *BRS* problem defined in (2). Thus, we have the following theorem.

Theorem 4: *BFRS* problem is NP-hard.

The biggest challenge for solving the *BFRS* problem is that the route scheduling of any EV is not independent because if an EV has been scheduled to be charged by a bus at a road segment, the other EVs cannot be scheduled to be charged by the same bus at the same road segment. So the method of finding routes for every EV in sequence is not valid for *BFRS* problem.

Considering the potential conflict when assigning a charging road segment to EV, we use the matching approach to solve the *BFRS* problem. The basic idea is that find all paths from the source to the destination for each EV subject to the time constraint, and then find a matching between the EVs and the charging road segments in the paths with maximum residual energy.

Algorithm 2 *FRSA*

Input: $\mathcal{G}$, $\{t_e, E_e^0, s_e, d_e, \gamma_e\}_{\forall e\in\mathcal{V}}$, $\{\mathcal{A}_b, r_b\}_{\forall b\in\mathcal{B}}$, ϵ, K, $\{r_e^a, t_b^a\}_{\forall e\in\mathcal{V},\ \forall a\in\mathcal{A},\forall b\in\mathcal{B}}$;
Output: $\mathcal{P}$;
// Phase 1: Bigraph Construction
$\mathcal{P} \leftarrow \varnothing$; $\mathcal{G}_2 \leftarrow \varnothing$;
foreach $e \in \mathcal{V}$ **do**
  // Case 1:
  $p_e \leftarrow SEA(\mathcal{G}, t_e, \epsilon, s_e, d_e)$;
  if $c(p_e) \le E_e^0$ **then** $\mathcal{G}_2 \leftarrow \mathcal{G}_2 \cup (e, p_e, E_e^0 - c(p_e))$;
  // Case 2:
  $\mathcal{P}_e^K \leftarrow KCSP(\mathcal{G}, t_e, K, s_e, d_e)$;
  foreach $p_e \in \mathcal{P}_e^K$ **do**
    foreach $b \in \mathcal{B}$ **do**
      if $p_e \cap \mathcal{A}_b \ne \varnothing$ **then**
        foreach $a_e^b \in p_e \cap \mathcal{A}_b$ **do**
          let $p_e(a,b)$ denote the route of e charged by b at road segment a;
          if $\Pi_{a\in p_e(a,b)} E_e^a \ge 0$ **and** $\sum_{a\in\overleftarrow{p_e}(a,b)} \frac{|a|}{r_e^a} \le t_b^{a_e^b}$ **and** $\sum_{a\in\overrightarrow{p_e}(a,b)} \frac{|a|}{r_e^a} \le t_e - t_b^{a_e^b} - \frac{|a_e^b|}{r_b}$ **then**
            $\mathcal{G}_2 \leftarrow \mathcal{G}_2 \cup \{(e, a_e^b, E_e^0 - c(p_e(a,b)))\}$;
  // Phase 2: Matching
  $\mathcal{M} \leftarrow Hungarian(\mathcal{G}_2)$;
  foreach $m \in \mathcal{M}$ **do**
    if $m = (e, p_e)$ **then** $\mathcal{P} \leftarrow \mathcal{P} \cup \{p_e\}$;
    if $m = (e, a_e^b)$ **then** $\mathcal{P} \leftarrow \mathcal{P} \cup \{p_e(a,b)\}$;

However, enumerating all possible time constrained paths for an EV will take exponential time. To make the problem tractable, we find the top K shortest paths from the source to the destination before deadline for each EV e. This problem is an instance of *K Constrained Shortest Path (KCSP)* problem [36]. Let $\mathcal{P}_e$ be the set of all feasible paths for each EV e from s_e to d_e before deadline t_e. The objective of *KCSP* problem is to find a subset $\mathcal{P}_e^K \subseteq \mathcal{P}_e$ of size K such that the length of each path in P_e^K is not larger than any path in $\mathcal{P}_e \setminus \mathcal{P}_e^K$. The *KCSP* problem of each EV e can be defined as follows:

$$\begin{aligned} &\boldsymbol{KCSP}\ \text{finding the subset } \mathcal{P}_e^K \subseteq \mathcal{P}_e \\ &s.t.\ (a)\ |p_e| \le |p_e'|, \forall p_e \in \mathcal{P}_e^K, \forall p_e' \in \mathcal{P}_e \setminus \mathcal{P}_e^K \\ &\quad (b)\ \textstyle\sum_{a\in p_e} \frac{|a|}{r_e^a} \le t_e, \forall p_e \in \mathcal{P}_e^K \\ &\quad (c)\ |\mathcal{P}_e^K| = K, \forall e \in \mathcal{V} \end{aligned} \tag{9}$$

As illustrated in Algorithm 2, *FRSA* consists of bigraph construction phase and matching phase.

In the bigraph construction phase, we consider the following two cases:

Case 1: The EV does not pass through the charging road segment. In this case, we compute the shortest path from the

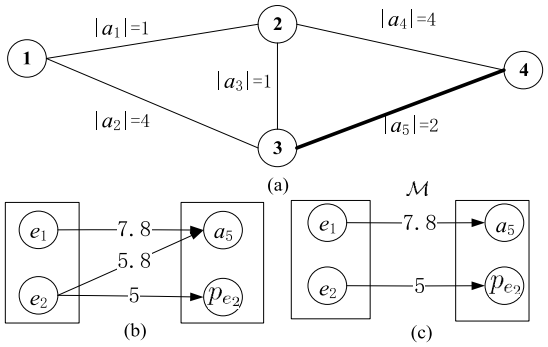

Fig. 2. Illustration of *FRSA*.

source to the destination before deadline for each EV. This also can be solved by *SEA* (Line 3). If the path satisfies the energy constraint, we add the triple $(e, p_e, E_e^0 - c(p_e))$ into the bigraph $\mathcal{G}_2$ (Line 4), where e and p_e are the vertexes in the two sides of the bigraph, and $E_e^0 - c(p_e)$ is the weight (residual energy) on the edge of (e, p_e).

Case 2: The EV passes through one charging road segment. Find the top K shortest paths from the source to the destination before deadline for each EV e by calling *KCSP*( ) (Line 5). For each selected path, we iterate all possible charging road segment a_e^b of the path for bus b. Let $p_e(a, b)$ denote the path of e charged by b at road segment a. We denote $\overleftarrow{p_e}(a, b)$ and $\overrightarrow{p_e}(a, b)$ as the sub-paths of $p_e(a, b)$ ahead of and behind the charging road segment a_e^b, respectively. We add the triple $(e, a_e^b, E_e^0 - c(p_e(a, b)))$ into the bigraph $\mathcal{G}_2$ (Line 12) if the following three conditions can be satisfied (Line 11): (1) the energy constraint can be satisfied for each road segment in path $p_e(a, b)$; (2) the EV e can drive into the charging road segment before the bus; and (3) the EV e can arrive the destination before the deadline after the charging.

In the matching phase, we find the maximum weighted matching on $\mathcal{G}_2$ to maximize the residual energy of all EVs. This can be solved by *Hungarian Algorithm* [37] (Line 13). For any EV e, if it is matched by p_e, put p_e into the final schedule $\mathcal{P}$; otherwise, if it is matched by a_e^b, put $p_e(a, b)$ into the final schedule $\mathcal{P}$ (Lines 14-16).

We use the example in Fig. 2 to illustrate how the Algorithm 2 works. In $\mathcal{G}$ shown in Fig. 2 (a), there are 4 road junctions and 5 road segments along with bus b and EVs e_1, e_2. $\gamma_{e_1} = \gamma_{e_2} = 1$. The speed of e_1 and e_2 at each road segment are listed as follows: $r_{e_1}^{a_1} = r_{e_2}^{a_1} = 0.5, r_{e_1}^{a_2} = r_{e_2}^{a_2} = 2, r_{e_1}^{a_3} = r_{e_2}^{a_3} = 0.5, r_{e_1}^{a_4} = r_{e_2}^{a_4} = 2$, and $r_{e_1}^{a_5} = r_{e_2}^{a_5} = 1$. So, the time of e_1 and e_2 traveling each road segment are 2. We set $s_{e_1} = 2, d_{e_1} = 4, t_{e_1} = 4$, $E_{e_1}^0 = 9$, $s_{e_2} = 1, d_{e_2} = 4, t_{e_2} = 4$ and $E_{e_2}^0 = 10$. We set $\mathcal{A}_b = \{a_5\}$, $\alpha = 0.9$, $t_b^{a_5} = 2$ and $r_b = 1$. So, the charging energy from bus b is 1.8.

Phase 1: Bigraph Construction

Case 1: The shortest paths from the source to the destination before deadline for e_1 and e_2 are $p_{e_1} = \{a_3, a_5\}$ and $p_{e_2} = \{a_1, a_4\}$, respectively. $c(p_{e_1}) = 3$ and $c(p_{e_2}) = 5$. We add the triple $(e_1, p_{e_1}, 7.8)$ and $(e_2, p_{e_2}, 5)$ into the bigraph $\mathcal{G}_2$ because these paths satisfies the energy constraints.

Case 2: $K = 2$. Find top 2 shortest paths for e_1 and e_2. $\mathcal{P}_{e_1}^K = \{p_{e_1}, \{a_4\}\}$. $\mathcal{P}_{e_2}^K = \{p_{e_2}, \{a_2, a_5\}\}$. Let $p_{e_1}(a_5, b)$ and $p_{e_2}(a_5, b)$ denote the routes of e_1 and e_2 charged by bus b at road segment a_5, respectively. Note that $p_{e_1}(a_5, b) = \{a_3, a_5\}$ and $p_{e_2}(a_5, b) = \{a_2, a_5\}$. Then, we add the triple $(e_2, a_5, 5.8)$ into the bigraph $\mathcal{G}_2$. So, we construct a bipartite graph $\mathcal{G}_2$ as shown in Fig. 2 (b).

Phase 2: Matching

- We compute the maximum weighed matching $\mathcal{M}$ of $\mathcal{G}_2$ shown in Fig. 2 (c) by calling *Hungarian*($\mathcal{G}_2$).
- The final route schedule of EV e_1 and e_2 are path $p_{e_1}(a_5, b)$ and path p_{e_2}, respectively.

Theorem 5: *BFRS* can output the schedule in $O(K|\mathcal{V}|m \cdot \max\{n(\log\log n + \frac{1}{\epsilon}), (|\mathcal{V}| + m)^2\})$.

Proof: In Phase 1, finding the K constrained shortest path takes $O(K|\mathcal{V}|mn(\log\log n + \frac{1}{\epsilon}))$ time. Finding all possible charging road segment a_e^b takes $O(K|\mathcal{V}|m)$ time. In Phase 2, finding the maximum weighted matching takes $O((|\mathcal{V}| + m)^2\ K|\mathcal{V}|m)$ time. Thus, the time complexity of *BFRS* is $O(K|\mathcal{V}|m \cdot \max\{n(\log\log n + \frac{1}{\epsilon}), (|\mathcal{V}| + m)^2\})$. □

V. Numerical Experiments

In this section, we conduct extensive simulations to verify the performance of our proposed algorithms with different number of EVs $|\mathcal{V}|$, number of buses $|\mathcal{B}|$, initial energy of EVs E_e^0, and deadline of EVs $t_e, \forall e \in \mathcal{V}$.

A. Simulation Setup

We use the data of 'New York City Bus Data' [38], which includes the live data recorded from NYC Buses. This dataset is from the NYC MTA bus data stream service.

To compare the proposed algorithms with the optimal solutions, we select the bus routes from the dataset to create the small-scale transportation network and large-scale transportation network, respectively. We compute the length of road segments through Google map. The speed of EV e at road segment a is set to the maximum speed of buses which pass through the same road segment. We set a random number in the interval [10], [40] km/h as the speed of EV passing through a if there is no bus passing through a. Moreover, we found that the shorter length of road segment is, the less speeds of buses from the dataset are. The result is consistent with the practical scenario of urban traffic, i.e., there are more road segments in the heavy traffic areas than those of good traffic areas. Furthermore, we assume that the initial time of EV route schedule is 8:00 AM in our experiments. The other parameter settings of our simulations are listed in Table III.

In our simulations, we measure the average residual energy of EVs $\bar{E}_R$, average travel time of EVs $\bar{T}$, and route assignment ratio, where $\bar{E}_R = \frac{1}{|\mathcal{P}|}(\sum_{p_e \in \mathcal{P}} E_e^0 - c(p_e))$, $\bar{T} = \frac{1}{|\mathcal{P}|}\sum_{p_e \in \mathcal{P}}\sum_{a \in p_e} \frac{|a|}{r_e^a}$. Here, $|\mathcal{P}|$ denotes the number of paths in $\mathcal{P}$.

All the simulations were run on a cloud server ECS [39] with 12 core Intel Xeon Platinum 8269CY and 48 GB memory.

TABLE III
PARAMETER SETTINGS IN OUR EXPERIMENTS

Parameter	Value in small-scale network	Value in large-scale network
α	100 kW	100 kW
ϵ	0.5	0.5
s_e	[1,16]	[1,25]
d_e	[1,16]	[1,25]
E_e^0	15 kWh	25 kWh
E_e^{max}	45 kWh	45 kWh
γ_e	0.1 kWh/km	0.1 kWh/km
t_e	1.5 $hours$	3.0 $hours$
$\|\mathcal{B}\|$	5	25
K	2	5
$\|\mathcal{V}\|$	200	500
n	16	25

B. Benchmarks

Since there are no existing algorithms for EV route scheduling based on bus network assisted wireless charging, we develop three benchmark algorithms for comparison,

(1) *SEA*. The solution of Case 1 of *BRS* or *BFRS* problem.
(2) *OPT*. The optimal solution for *BRS* problem. *OPT* enumerates all the feasible paths of Case 1 and Case 2 of the *BRS* problem, and selects the path with maximal residual energy (minimum energy consumption) as the solution.
(3) *FOPT*. The optimal solution for *BFRS* problem. *FOPT* enumerates all the feasible paths of Case 1 and Case 2 in the bigraph construction phase. For the matching phase, *FOPT* uses the same process as that in *FRSA*.

C. Performance Evaluation for Small-Scale Network

In this subsection, we evaluate the performance of *SEA*, *RSA*, *OPT*, *FRSA* and *FOPT* in the small-scale network shown in Fig. 3. Table IV gives the schedules of bus lines in small-scale transportation network including sub routes, time when the bus enters road segment, route length, average travel time, and average speed of bus. The above information are calculated based on the data records from 8:00-13:00 AM on December 1-6, 2017.

Impact of number of EVs. We vary number of EVs $|\mathcal{V}|$ from 20 to 200. Fig. 4 shows that *RSA* reduces 7.89% of travel time and obtains 121.07% increase of residual energy of *SEA* on average, *FRSA* increases 45.99% of residual energy with 1.79% of extra travel time of *SEA* on average. This indicates that the proposed algorithms significantly outperforms *SEA*. This is because the output of *RSA* and *FRSA* is the better one of the path obtained by *SEA* and path with the minimum energy consumption via charging road segments. From Table I, the designed wireless charging system can provide amount of energy to EVs. In most cases, the average residual energy of paths from Case 2 of *RSA* and *FRSA* is larger than that of paths from Case 1 (computed by *SEA*). Moreover, the residual energy of *FRSA* is less than that of *RSA* because of avoiding the charging conflict. Thus, the length of route becomes larger as *FRSA* will assign a conflict-free route for each EV. The average residual energy of *RSA* and *FRSA* is 95.47% and

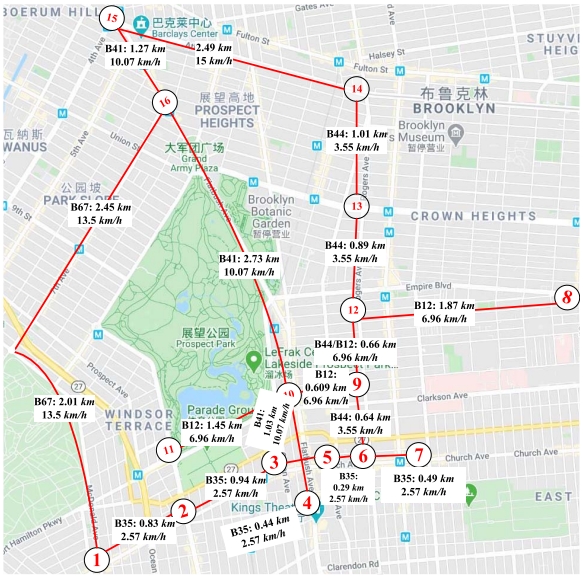

Fig. 3. Small-scale transportation network. The white nodes represent road junctions and the red lines represent road segments, respectively. There are three parameters on each road segment, i.e., bus ID, length of road segment and speed of EV passing through the road segment.

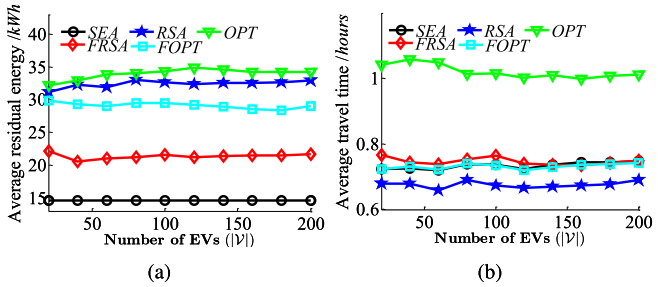

Fig. 4. Impact of number of EVs ($|\mathcal{V}|$): (a) Average residual energy *vs.* number of EVs. (b) Average travel time *vs.* number of EVs.

73.48% of those of *OPT* and *FOPT*, respectively. Note that the performance gap between *RSA* and *OPT* is small since *RSA* has the guaranteed approximation.

Impact of number of buses. We vary number of buses $|\mathcal{B}|$ from 2 to 5. Fig. 5 shows that *RSA* reduces 10.52% of travel time and increases 124.27% of residual energy of *SEA* on average, *FRSA* increases 68.82% of residual energy with 1.02% of extra travel time of *SEA* on average. Note that *RSA* reduces 20.53% of travel time and outputs 81.96% of residual energy of *OPT* on average, and *FRSA* can obtain 97.55% residual energy with 5.14% of extra travel time of *FOPT* on average, respectively. Fig. 5 (a) shows that average residual energy of *RSA*, *OPT*, *FRSA* and *FOPT* increase with $|\mathcal{B}|$. This is because there are more charging road segments, and more EVs can obtain the energy from the charging system.

Impact of initial energy of EVs. We vary initial energy of EVs E_e^0 from 15.5 kWh to 19 kWh. Fig. 6 shows that *RSA* reduces 11.75% of travel time and increases 34.21% of residual energy of *SEA* on average, *FRSA* increases 41.27% of residual energy with 0.44% of extra travel time of *SEA* on average. Note that *RSA* reduces 6.02% of travel time and outputs 53.15% of residual energy of *OPT* on average, and *FRSA* can obtain 84.08% residual energy with 4.79% of extra

TABLE IV
SCHEDULES OF BUS LINES IN SMALL-SCALE NETWORK

Bus ID	Sub route	Time when the bus enters road segment ($hours$)	Route length (km)	Average travel time ($hours$)	Average speed (km/h)
$B67$	$\{1 \to 16\}$	0.95	4.47	0.33	13.5
$B44$	$\{6 \to 9 \to 12 \to 13 \to 14\}$	{1.05, 1.15, 1.42, 1.95}	3.20	0.9	3.55
$B41$	$\{4 \to 10 \to 16 \to 15\}$	{1.45, 1.78, 1.83}	5.03	0.5	10.07
$B12$	$\{11 \to 10 \to 9 \to 12 \to 8\}$	{1.62, 1.95, 2.12, 2.28}	4.60	0.66	6.96
$B35$	$\{1 \to 2 \to 3 \to 5 \to 6 \to 7\}$	{1.12, 1.45, 1.95, 2.12, 2.28}	2.99	1.16	2.57

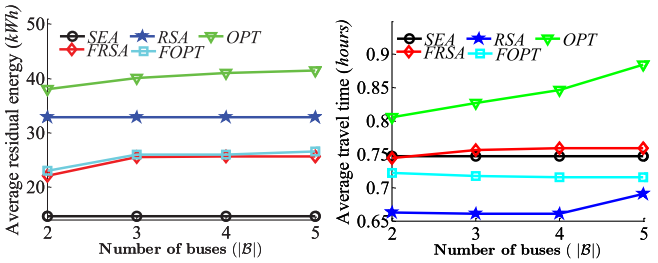

(a) (b)

Fig. 5. Impact of number of buses ($|\mathcal{B}|$): (a) Average residual energy *vs.* number of buses. (b) Average travel time *vs.* number of buses.

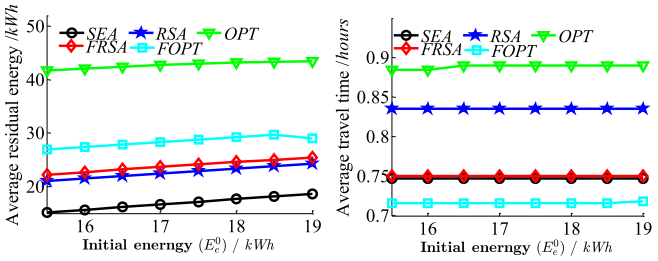

(a) (b)

Fig. 6. Impact of initial energy (E_e^0): (a) Average residual energy *vs.* initial energy. (b) Average travel time *vs.* initial energy.

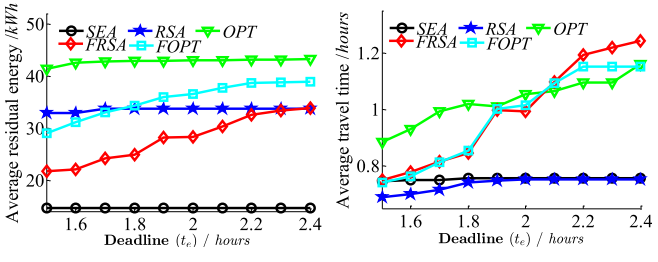

(a) (b)

Fig. 7. Impact of deadline (t_e): (a) Average residual energy *vs.* deadline. (b) Average travel time *vs.* deadline.

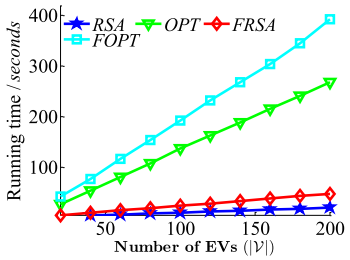

Fig. 8. Running time.

travel time of *FOPT* on average, respectively. Fig. 6 (a) shows that average residual energy for *RSA*, *OPT*, *FRSA* and *FOPT*

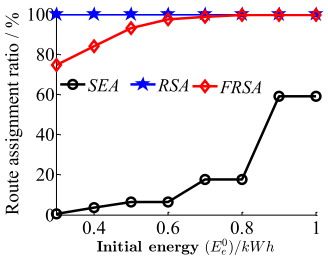

Fig. 9. Route assignment ratio.

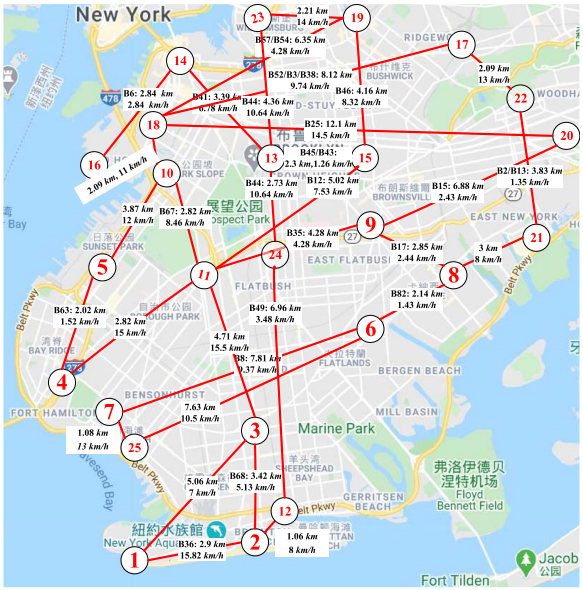

Fig. 10. Large-scale transportation network.

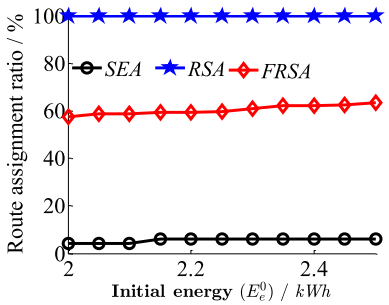

Fig. 11. Route assignment ratio.

increase with E_e^0. This is because the more initial energy, the better solution of Case 2.

Impact of deadline of EVs. We vary deadline of EVs t_e from 1.5 $hours$ to 2.4 $hours$. Fig. 7 shows that *RSA* reduces 2.46% of travel time and increases 128.59% of residual energy of *SEA* on average, *FRSA* increases 90.47% of residual energy with

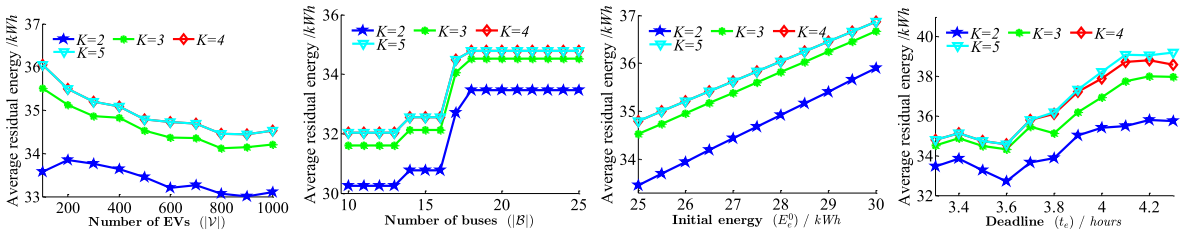

Fig. 12. Impact of K: (a) Average residual energy *vs.* number of EVs. (b) Average residual energy *vs.* number of buses. (c) Average residual energy *vs.* initial energy, (d) Average residual energy *vs.* deadline.

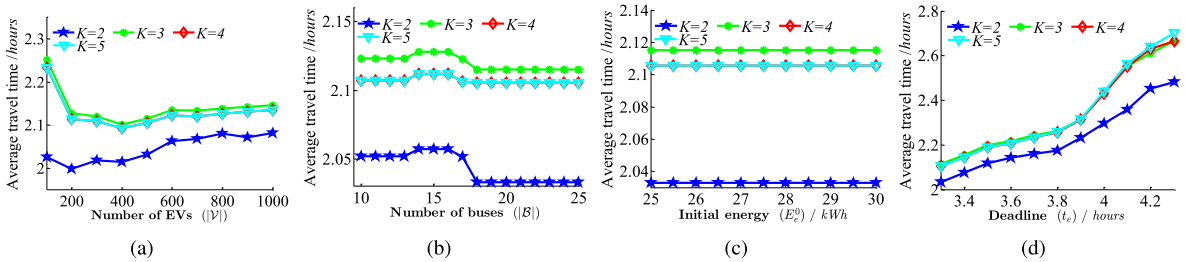

Fig. 13. Impact of K: (a) Average travel time *vs.* number of EVs. (b) Average travel time *vs.* number of buses. (c) Average travel time *vs.* initial energy, (d) Average travel time *vs.* deadline.

31.54% of extra travel time of *SEA* on average. Note that *RSA* reduces 28.55% of travel time and outputs 78.32% of residual energy of *OPT* on average, and *FRSA* can obtain 78.91% residual energy with 2.46% of extra travel time of *FOPT* on average, respectively. Fig. 7 (a) shows that average travel time of *RSA*, *OPT*, *FRSA* and *FOPT* increases with t_e. This is because with the generous deadline of EVs, *RSA* and *FRSA* can find the better charging road segment for each EV which can obtain more charging energy from the schedules of bus lines.

Overall, *RSA* and *FRSA* can significantly increase the average residual energy through the designed algorithms.

Running time. We vary $|\mathcal{V}|$ from 20 to 200. Fig. 8 shows that the running time of *RSA*, *OPT*, *FRSA* and *FOPT* grow linearly with the number of EVs. The running time of *OPT* and *FOPT* are 147.68 *seconds* and 211.70 *seconds* on average, respectively. Whereas, *RSA* and *FRSA* can complete the route schedule of all EVs in 10.84 *seconds* and 25.80 *seconds* on average, respectively. So, the proposed algorithms are much more suitable to the large-scale network.

Route assignment ratio. We vary initial energy E_e^0 from 0.3 kWh to 1 kWh. Fig. 9 shows that the route assignment ratio of *RSA* keeps 100%, and the route assignment ratio of *FRSA* and *SEA* increase with initial energy. Note that *RSA* and *FRSA* obtains 370.59% and 338.82% increase of route assignment ratio of *SEA* on average, respectively. This is because *SEA* can not find the feasible routes for 93.5% of EVs when their initial energy are less than 0.6 kWh in the small-scale transportation network. However, these EVs can find the feasible routes through the designed algorithms.

D. Performance Evaluation for Large-Scale Network

In this subsection, we evaluate the performance of *SEA*, *RSA*, and *FRSA* in the large-scale transportation network as shown in Fig. 10. Table V gives the schedules of bus lines in the large-scale transportation network.

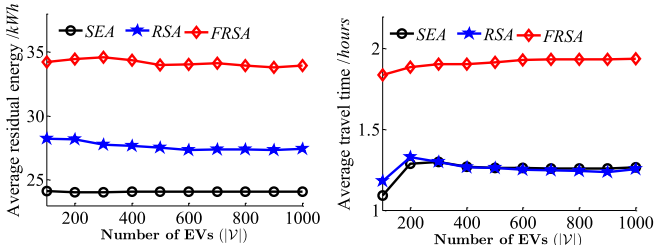

Fig. 14. Impact of number of EVs ($|\mathcal{V}|$): (a) Average residual energy *vs.* number of EVs. (b) Average travel time *vs.* number of EVs.

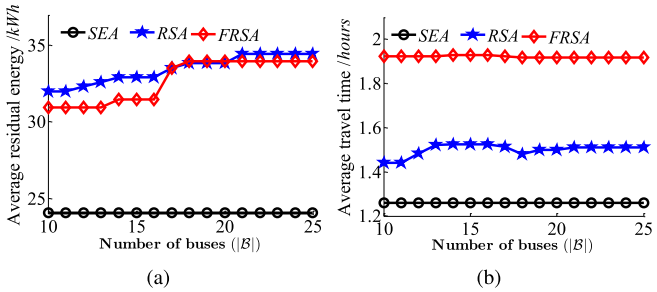

Fig. 15. Impact of number of buses ($|\mathcal{B}|$): (a) Average residual energy *vs.* number of buses. (b) Average travel time *vs.* number of buses.

Route assignment ratio. We vary initial energy E_e^0 from 2 kWh to 2.5 kWh. Fig. 11 shows that the route assignment ratio of *RSA* keeps 100%, and the route assignment ratio of *FRSA* and *SEA* increases with initial energy. Note that *RSA* and *FRSA* obtain 1668.49% and 967.52% increase of route assignment ratio of *SEA* on average, respectively.

Impact of K. We evaluate the performance of *FRSA* when K is changed from 2 to 5, with different number of EVs, number of buses, initial energy, and deadline. Fig. 12 and Fig. 13

TABLE V
SCHEDULES OF BUS LINES IN LARGE-SCALE NETWORK

Bus ID	Sub route	Time when the bus enters road segment ($hours$)	Route length (km)	Average travel time ($hours$)	Average speed (km/h)
$B67$	$\{10 \rightarrow 11\}$	0.95	2.82	0.33	8.46
$B44$	$\{23 \rightarrow 13 \rightarrow 24\}$	{1.45, 1.95}	7.09	0.67	10.635
$B41$	$\{13 \rightarrow 14\}$	1.45	3.39	0.5	6.78
$B12$	$\{11 \rightarrow 15\}$	1.62	5.02	0.67	7.53
$B35$	$\{9 \rightarrow 11\}$	1.45	4.28	1	4.28
$B6$	$\{14 \rightarrow 16\}$	2.78	2.84	1	2.84
$B17$	$\{8 \rightarrow 9\}$	2.62	2.85	1	2.44
$B82$	$\{6 \rightarrow 8\}$	2.62	2.14	1.5	1.43
$B52$	$\{17 \rightarrow 18\}$	2.62	8.12	1	8.12
$B46$	$\{15 \rightarrow 19\}$	2.12	4.1	0.5	8.32
$B68$	$\{2 \rightarrow 3\}$	2.12	3.42	0.67	5.13
$B2$	$\{21 \rightarrow 22\}$	2.12	3.83	2.84	1.35
$B15$	$\{9 \rightarrow 20\}$	2.78	6.88	2.83	2.43
$B8$	$\{6 \rightarrow 7\}$	2.78	7.81	0.83	9.37
$B13$	$\{21 \rightarrow 22\}$	2.28	3.83	1	0.28
$B3$	$\{17 \rightarrow 18\}$	2.12	8.12	0.83	9.74
$B25$	$\{18 \rightarrow 20\}$	2.96	12.1	0.83	14.5
$B57$	$\{18 \rightarrow 19\}$	2.96	6.35	0.87	7.26
$B45$	$\{13 \rightarrow 15\}$	2.43	2.3	1.83	1.26
$B63$	$\{4 \rightarrow 5\}$	2.95	2.02	1.33	1.52
$B49$	$\{12 \rightarrow 24\}$	2.78	6.96	2	3.48
$B54$	$\{18 \rightarrow 19\}$	2.62	6.96	2	4.28
$B36$	$\{1 \rightarrow 2\}$	2.62	2.9	0.18	15.82
$B43$	$\{13 \rightarrow 15\}$	2.62	2.3	0.33	6.9
$B38$	$\{17 \rightarrow 18\}$	2.82	8.12	0.33	8.12

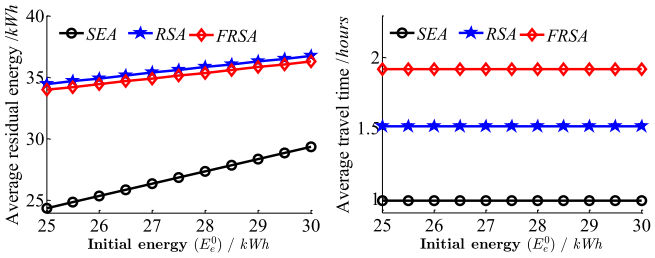

(a) (b)

Fig. 16. Impact of initial energy (E_e^0): (a) Average residual energy *vs.* initial energy. (b) Average travel time *vs.* initial energy.

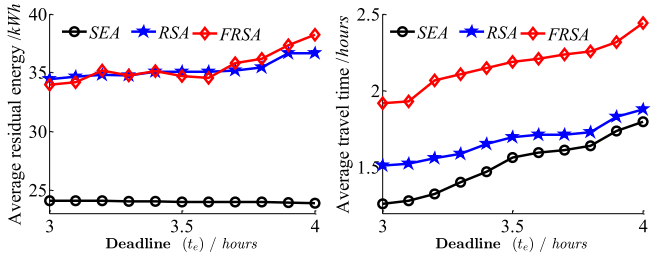

(a) (b)

Fig. 17. Impact of deadline (t_e): (a) Average residual energy *vs.* deadline. (b) Average travel time *vs.* deadline.

show that both average residual energy and average travel time become stable when K exceeds 4. This is because K is large enough for *FRSA* to find the feasible routes for all EVs.

Fig. 14, Fig. 15, Fig. 16, and Fig. 17 indicate that the proposed algorithms can achieve much better performance in terms of average residual energy than *SEA* in large-scale transportation network. This indicates that the proposed algorithms have good scalability. Moreover, *RSA* increases 33.27% of residual energy with 20.79% of extra travel time of *SEA* on average. Furthermore, *FRSA* increases 39.07% of residual energy with 60.59% of extra travel time of *SEA* on average.

VI. CONCLUSION AND FUTURE WORK

In this article, we have designed the unique wireless charging system for EVs supported by the bus network in urban areas. The buses are charged by the OLEV system, and equipped with the directed transmitting antennas of MPT. The EVs are charged by the MPT when they are close enough to the buses. We have formulated *BRS* problem to maximize the total residual energy subject to all EVs can arrive to their destinations before deadlines, and proposed an approximation algorithm based on the approximation solution of *RSP* problem. To avoid the charging conflict and relieve traffic congestions, we have further formulated *BFRS* problem and proposed a polynomial-time algorithm by solving the *KCSP* problem and the maximum weighted matching between the EVs and the candidate routes. The efficiency of the proposed algorithms have been confirmed by both of the theoretical analysis and numerical simulations. The simulation results show that *RSA* and *FRSA* can increase the average residual energy by 67.66% and 50.36% through the designed charging system. Moreover, *RSA* reduces 22.22% of travel time and outputs 77.23% of residual energy of *OPT*, and *FRSA* can obtain 83.51% residual energy with 3.62% of extra travel time of *FOPT* on average, respectively. Furthermore, *RSA* and *FRSA* can increase the route assignment ratio by 1019.50% and 653.17% compared with the solution without the designed wireless charging system.

In the future, we plan to extend this work to enable each EV to be charged more than once during their journeys. In addition, insufficient traffic capacity and/or traffic

infrastructure may cause the recurrent congestion at some fixed road junctions or road segments during morning or afternoon rush hours [40]. Then, the speed of buses and EVs will be uncertain. Thus, we plan to design a recurrent congestion analysis pattern based on 5G and edge intelligent system to predict the real time speed of EVs and buses, for improving the accuracy of synchronization between EVs and buses.

REFERENCES

[1] *China YiWei Institute of Economics*. Accessed: Mar. 2020. [Online]. Available: http://www.evtank.cn

[2] *Fuji Keizai Group*. Accessed: Mar. 2020. [Online]. Available: https://www.fuji-keizai.co.jp

[3] W. Shuai, P. Maille, and A. Pelov, "Charging electric vehicles in the smart city: A survey of economy-driven approaches," *IEEE Trans. Intell. Transp. Syst.*, vol. 17, no. 8, pp. 2089–2106, Aug. 2016.

[4] Q. Wang, X. Liu, J. Du, and F. Kong, "Smart charging for electric vehicles: A survey from the algorithmic perspective," *IEEE Commun. Surveys Tuts.*, vol. 18, no. 2, pp. 1500–1517, 2nd Quart., 2016.

[5] S. Y. Choi, B. W. Gu, S. Y. Jeong, and C. T. Rim, "Advances in wireless power transfer systems for roadway-powered electric vehicles," *IEEE J. Emerg. Sel. Topics Power Electron.*, vol. 3, no. 1, pp. 18–36, Mar. 2015.

[6] Y. D. Ko and Y. J. Jang, "The optimal system design of the online electric vehicle utilizing wireless power transmission technology," *IEEE Trans. Intell. Transp. Syst.*, vol. 14, no. 3, pp. 1255–1265, Sep. 2013.

[7] H. Toromura, Y. Huang, S. Koyama, J. Miyakoshi, and N. Shinohara, "Biological effects of high-power microwave power transfer for electric vehicle," in *Proc. IEEE Wireless Power Transf. Conf. (WPTC)*, May 2016, pp. 1–3.

[8] *Tesla*. Accessed: Mar. 2020. [Online]. Available: https://www.tesla.com/supercharger

[9] L. L. Hatfield and B. Schilder, "Microwave shielding measurement method," in *Proc. IEEE Pulsed Power Conf.*, Jun. 2009, pp. 1280–1284.

[10] M. Sachenbacher, M. Leucker, and A. Haselmayr, "Efficient energy-optimal routing for electric vehicles," in *Proc. 25th AAAI Conf. Artif. Intell.*, 2011, pp. 1402–1407.

[11] A. M. Bozorgi, M. Farasat, and A. Mahmoud, "A time and energy efficient routing algorithm for electric vehicles based on historical driving data," *IEEE Trans. Intell. Vehicles*, vol. 2, no. 4, pp. 308–320, Dec. 2017.

[12] Z. Sun, X. Zhou, J. Du, and X. Liu, "When traffic flow meets power flow: On charging station deployment with budget constraints," *IEEE Trans. Veh. Technol.*, vol. 66, no. 4, pp. 2915–2926, Apr. 2017.

[13] H. Gao, C. Liu, Y. Li, and X. Yang, "V2 VR: Reliable hybrid-network-oriented V2 V data transmission and routing considering RSUs and connectivity probability," *IEEE Trans. Intell. Transp. Syst.*, early access, Apr. 13, 2020, doi: 10.1109/TITS.2020.2983835.

[14] H. Gao, W. Huang, and X. Yang, "Applying probabilistic model checking to path planning in an intelligent transportation system using mobility trajectories and their statistical data," *Intell. Automat. Soft Comput.*, vol. 25, no. 3, pp. 547–559, 2019.

[15] L. Kuang, C. Hua, J. Wu, Y. Yin, and H. Gao, "Traffic volume prediction based on multi-sources GPS trajectory data by temporal convolutional network," *ACM/Springer Mobile Netw. Appl.*, vol. 25, pp. 1405–1417, Feb. 2020, doi: 10.1007/s11036-019-01458-6.

[16] Y. Zhang, P. You, and L. Cai, "Optimal charging scheduling by pricing for EV charging station with dual charging modes," *IEEE Trans. Intell. Transp. Syst.*, vol. 20, no. 9, pp. 3386–3396, Sep. 2019.

[17] H. Chen, Z. Hu, H. Luo, J. Qin, R. Rajagopal, and H. Zhang, "Design and planning of a multiple-charger multiple-port charging system for PEV charging station," *IEEE Trans. Smart Grid*, vol. 10, no. 1, pp. 173–183, Jan. 2019.

[18] Z. Moghaddam, I. Ahmad, D. Habibi, and Q. V. Phung, "Smart charging strategy for electric vehicle charging stations," *IEEE Trans. Transport. Electrific.*, vol. 4, no. 1, pp. 76–88, Mar. 2018.

[19] Z. Khan, S. M. Khan, M. Chowdhury, I. Safro, and H. Ushijima-Mwesigwa, "Wireless charging utility maximization and intersection control delay minimization framework for electric vehicles," *Comput.-Aided Civil Infrastruct. Eng.*, vol. 34, no. 7, pp. 547–568, Jul. 2019.

[20] Y. D. Ko and Y. J. Jang, "The optimal system design of the online electric vehicle utilizing wireless power transmission technology," *IEEE Trans. Intell. Transp. Syst.*, vol. 14, no. 3, pp. 1255–1265, Sep. 2013.

[21] C.-H. Ou, H. Liang, and W. Zhuang, "Investigating wireless charging and mobility of electric vehicles on electricity market," *IEEE Trans. Ind. Electron.*, vol. 62, no. 5, pp. 3123–3133, May 2015.

[22] B. Esteban, M. Sid-Ahmed, and N. C. Kar, "A comparative study of power supply architectures in wireless EV charging systems," *IEEE Trans. Power Electron.*, vol. 30, no. 11, pp. 6408–6422, Nov. 2015.

[23] Y. Gao, C. Duan, A. A. Oliveira, A. Ginart, K. B. Farley, and Z. T. H. Tse, "3-D coil positioning based on magnetic sensing for wireless EV charging," *IEEE Trans. Transport. Electrific.*, vol. 3, no. 3, pp. 578–588, Sep. 2017.

[24] S. D. Manshadi, M. E. Khodayar, K. Abdelghany, and H. Uster, "Wireless charging of electric vehicles in electricity and transportation networks," *IEEE Trans. Smart Grid*, vol. 9, no. 5, pp. 4503–4512, Sep. 2018.

[25] Y. He, B. Venkatesh, and L. Guan, "Optimal scheduling for charging and discharging of electric vehicles," *IEEE Trans. Smart Grid*, vol. 3, no. 3, pp. 1095–1105, Sep. 2012.

[26] Y. Cao *et al.*, "Mobile edge computing for big data-enabled electric vehicle charging," *IEEE Commun. Mag.*, vol. 56, no. 3, pp. 150–156, Mar. 2018.

[27] X. Tang, S. Bi, and Y.-J.-A. Zhang, "Distributed routing and charging scheduling optimization for Internet of electric vehicles," *IEEE Internet Things J.*, vol. 6, no. 1, pp. 136–148, Feb. 2019.

[28] M. Ammous, S. Belakaria, S. Sorour, and A. Abdel-Rahim, "Optimal cloud-based routing with in-route charging of Mobility-on-Demand electric vehicles," *IEEE Trans. Intell. Transp. Syst.*, vol. 20, no. 7, pp. 2510–2522, Jul. 2019.

[29] C. Liu, M. Zhou, J. Wu, C. Long, and Y. Wang, "Electric vehicles en-route charging navigation systems: Joint charging and routing optimization," *IEEE Trans. Control Syst. Technol.*, vol. 27, no. 2, pp. 906–914, Mar. 2019.

[30] O. Ardakanian, C. Rosenberg, and S. Keshav, "Distributed control of electric vehicle charging," in *Proc. ACM 4th Int. Conf. Future Energy Syst.*, 2013, pp. 101–112.

[31] A. Zakariazadeh, S. Jadid, and P. Siano, "Multi-objective scheduling of electric vehicles in smart distribution system," *Energy Convers. Manage.*, vol. 79, pp. 43–53, Mar. 2014.

[32] V. T. Tran, M. R. Islam, K. M. Muttaqi, and D. Sutanto, "An efficient energy management approach for a solar-powered EV battery charging facility to support distribution grids," *IEEE Trans. Ind. Appl.*, vol. 55, no. 6, pp. 6517–6526, Nov. 2019.

[33] S. Jeong, Y. J. Jang, and D. Kum, "Economic analysis of the dynamic charging electric vehicle," *IEEE Trans. Power Electron.*, vol. 30, no. 11, pp. 6368–6377, Nov. 2015.

[34] R. Hassin, "Approximation schemes for the restricted shortest path problem," *Math. Oper. Res.*, vol. 17, no. 1, pp. 36–42, Feb. 1992.

[35] D. H. Lorenz and D. Raz, "A simple efficient approximation scheme for the restricted shortest path problem," *Oper. Res. Lett.*, vol. 28, no. 5, pp. 213–219, Jun. 2001.

[36] N. Shi, "K constrained shortest path problem," *IEEE Trans. Autom. Sci. Eng.*, vol. 7, no. 1, pp. 15–23, Jan. 2010.

[37] J. Munkres, "Algorithms for the assignment and transportation problems," *J. Soc. for Ind. Appl. Math.*, vol. 5, no. 1, pp. 32–38, Mar. 1957.

[38] (Mar. 2020). *New York City Bus Data*. [Online]. Available: https://www.kaggle.com/stoney71/new-york-city-transport-statistics/

[39] (Mar. 2020). *Aliyun ECS Cloud Server*. [Online]. Available: https://www.aliyun.com/product/ecs

[40] S. An, H. Yang, J. Wang, N. Cui, and J. Cui, "Mining urban recurrent congestion evolution patterns from GPS-equipped vehicle mobility data," *Inf. Sci.*, vol. 373, pp. 515–526, Dec. 2016.

Yong Jin received the M.S. degree from Nanjing Tech University, Nanjing, China, in 2009. He is currently pursuing the Ph.D. degree with the Jiangsu Key Laboratory of Big Data Security and Intelligent Processing, Nanjing University of Posts and Telecommunications, Nanjing. He is an Associate Professor with the School of Computer Science and Engineering, Changshu Institute of Technology, Changshu, China. His current research interests include wireless charging and intelligent transportation systems.

Jia Xu (Member, IEEE) received the M.S. degree from the School of Information and Engineering, Yangzhou University, Jiangsu, China, in 2006, and the Ph.D. degree from the School of Computer Science and Engineering, Nanjing University of Science and Technology, Jiangsu, in 2010. He was a Visiting Scholar with the Department of Electrical Engineering and Computer Science, Colorado School of Mines, from November 2014 to May 2015. He is currently a Professor with the School of Computer Science, Nanjing University of Posts and Telecommunications. His main research interests include crowdsourcing, edge computing, and wireless sensor networks. He has served as the PC Co-Chair of SciSec 2019, the Organizing Chair of ISKE 2017, a TPC Member of GLOBECOM, ICC, MASS, ICNC, and EDGE. He serves as the Publicity Co-Chair of SciSec 2021.

Sixu Wu received the bachelor's degree from the School of Computer Science, Nanjing University of Posts and Telecommunications, Nanjing, China, in 2019, where he is currently pursuing the master's degree with the Jiangsu Key Laboratory of Big Data Security and Intelligent Processing. His research interests include mobile crowd sensing and wireless charger networks.

Lijie Xu received the Ph.D. degree from the Department of Computer Science and Technology, Nanjing University, Nanjing, in 2014. He was a Research Assistant with the Department of Computing, The Hong Kong Polytechnic University, Hong Kong, from 2011 to 2012. He is currently an Associate Professor with the Jiangsu Key Laboratory of Big Data Security and Intelligent Processing, Nanjing University of Posts and Telecommunications, Nanjing. His research interests mainly include wireless sensor networks, ad-hoc networks, mobile and distributed computing, and graph theory algorithms.

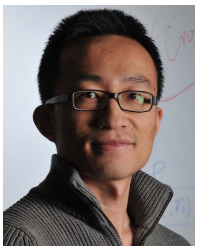

Dejun Yang (Senior Member, IEEE) received the B.S. degree in computer science from Peking University, Beijing, China, in 2007, and the Ph.D. degree in computer science from Arizona State University, Tempe, AZ, USA, in 2013. He is currently an Associate Professor of computer science with the Colorado School of Mines, Golden, CO, USA. His research interests include the Internet of Things, networking, and mobile sensing and computing with a focus on the applications of game theory, optimization, algorithm design, and machine learning to resource allocation, security, and privacy problems. He received the IEEE Communications Society William R. Bennett Prize in 2019 (Best Paper Award for the IEEE/ACM TRANSACTIONS ON NETWORKING (TON) and the IEEE TRANSACTIONS ON NETWORK AND SERVICE MANAGEMENT in the previous three years), Best Paper Awards at the IEEE Global Communications Conference (GLOBECOM) in 2015, the IEEE International Conference on Mobile Ad Hoc and Sensor Systems in 2011, and the IEEE International Conference on Communications (ICC) in 2011 and 2012, and the Best Paper Award Runner-Up at the IEEE International Conference on Network Protocols (ICNP) in 2010. He has served as the TPC Vice-Chair of *Information Systems* for the IEEE International Conference on Computer Communications (INFOCOM) and serves as an Associate Editor for the IEEE INTERNET OF THINGS JOURNAL (IoT-J).